JOURNAL OF THE ROYAL SOCIETY Interface

rsif.royalsocietypublishing.org

Research

Cite this article: Irmscher M, de Jong AM, Kress H, Prins MWJ. 2013 A method for time-resolved measurements of the mechanics of phagocytic cups. J R Soc Interface 10: 20121048.
http://dx.doi.org/10.1098/rsif.2012.1048

Received: 20 December 2012
Accepted: 11 February 2013

Subject Areas:
biophysics

Keywords:
magnetic micromanipulation, phagocytosis, particles, membrane, cell mechanics

Authors for correspondence:
Holger Kress
e-mail: holger.kress@uni-bayreuth.de
Menno W. J. Prins
e-mail: m.w.j.prins@tue.nl

Electronic supplementary material is available at http://dx.doi.org/10.1098/rsif.2012.1048 or via http://rsif.royalsocietypublishing.org.

Royal Society Publishing
Informing the science of the future

A method for time-resolved measurements of the mechanics of phagocytic cups

Matthias Irmscher[1], Arthur M. de Jong[1], Holger Kress[1,2] and Menno W. J. Prins[1,3]

[1]Department of Applied Physics, Eindhoven University of Technology, Eindhoven, The Netherlands
[2]Experimental Physics I, University of Bayreuth, Bayreuth, Germany
[3]Philips Research, Eindhoven, The Netherlands

The internalization of matter by phagocytosis is of key importance in the defence against bacterial pathogens and in the control of cancerous tumour growth. Despite the fact that phagocytosis is an inherently mechanical process, little is known about the forces and energies that a cell requires for internalization. Here, we use functionalized magnetic particles as phagocytic targets and track their motion while actuating them in an oscillating magnetic field, in order to measure the translational and rotational stiffnesses of the phagocytic cup as a function of time. The measured evolution of stiffness reveals a characteristic pattern with a pronounced peak preceding the finalization of uptake. The measured stiffness values and their time dependence can be interpreted with a model that describes the phagocytic cup as a pre-stressed membrane connected to an elastically deformable actin cortex. In the context of this model, the stiffness peak is a direct manifestation of a previously described mechanical bottleneck, and a comparison of model and data suggests that the membrane advances around the particle at a speed of about 20 nm s^{-1}. This approach is a novel way of measuring the progression of emerging phagocytic cups and their mechanical properties *in situ* and in real time.

1. Introduction

The ability of cells to bind and ingest objects by a process called phagocytosis is a highly conserved mechanism, and can be found in a variety of different systems [1]. While unicellular organisms perform phagocytosis to take up nutrients [2], the process is mostly known as a key feature of the innate immune system of higher order organisms. Several types of immune cells are capable of carrying out phagocytosis, but specialized white blood cells called phagocytes are most effective.

In the course of phagocytosis, potentially harmful objects such as bacteria, apoptotic cells or foreign particles larger than about 0.5 µm [3,4] are first identified via native or acquired molecular patterns on their surfaces that allow immune cells to bind them. Depending on the ligand–receptor interaction, a specific signalling cascade then triggers a directed and localized deformation of the membrane with the aim of internalizing the bound object. A variety of molecules have been shown to function as phagocytic markers [4], which most prominently complement and crystalline fragments (Fc regions) of immunoglobulins [5]. The latter are bound by Fc receptors (FcR) whose structures are conserved across the different cell types that express them. Interestingly, genetic transfection of FcR has been shown to enable phagocytosis, even in cell lines that normally lack the receptor [6]. Owing to its robust and unambiguous response, FcR-mediated phagocytosis remains the most frequently studied mechanism by which cells recognize and internalize external objects.

During the engulfment phase, the cell membrane is deformed such that the interaction area with the phagocytic target increases and a so-called phagocytic

cup is formed. In the case of FcR-mediated phagocytosis, the membrane deformations are made permanent by new bonds that are formed in a zipper-like fashion [7]. As the membrane is protruding, the ligation of additional receptors triggers the localized polymerization of actin filaments that provide a stabilizing scaffold. The engulfment of the particle is finalized when the membrane closes in on itself, at which point the phagocytic target is entirely surrounded by an envelope comprising a lipid double layer and the previously formed actin shell [8]. This object, called a phagosome, subsequently undergoes a sequence of steps that are aimed at destroying its contents by acidification and enzymatic digestion.

The actin-dependent reorganization of the membrane during the formation of a phagocytic cup is an inherently mechanical process [9,10]. The deformation of the membrane is governed by mechanical parameters such as the cortical tension and the bending stiffness of the cell membrane [11]. Depending on the size of the object, engulfing the phagocytic target may require the mobilization of excess membrane that can be provided through the unwrapping of membrane folds [11,12]. The shape and orientation of the phagocytic target [9,10] as well as its elastic stiffness [13] have been shown to have an influence on the effectiveness of phagocytosis. All of these parameters are defined on a larger scale than the molecular processes that drive phagocytosis, and many questions regarding the bridging of these scales remain unanswered.

In a classic experiment, the cortical tension of a phagocyte is measured dynamically by holding a non-adherent neutrophil in a micropipette at constant suction pressure while presenting it with a suitable phagocytic target [14]. These experiments have shown that the engulfment of a medium-sized target coincides with an increase in cortical tension as the cell membrane stretches and excess membrane is released from wrinkles [11]. The trajectory of the target during ingestion has been found to depend on its coating, indicating that molecular recognition triggers distinct modes of force generation [15]. Despite the insights the micropipetting approach has provided, it has the disadvantage that a connection is made between a globally measured quantity and a highly localized cellular process.

Micro-particles are uniquely suited to measure forces at the site of phagocytosis. Particles in a weak optical trap have been used as phagocytic bait to reveal that protruding filopodia pull targets closer in discrete steps [16]. During this initial stage of phagocytosis, optical tweezers are most useful owing to their force resolution of the order of piconewtons. At a later stage, when the particle is in the process of being wrapped by the protruding membrane, the energy gained by the formation of multiple bonds supersedes the interaction energy between the particle and the optical trap. In this regime, discernible displacements can only be produced by methods such as magnetic tweezers or atomic force microscopes. While both the initial transport of particles by retracting filopodia [16,17] and the viscoelastic environment of phagosomes [18–20] have been characterized in mechanical terms, measurements of the forces that drive the formation of the phagocytic cup remain elusive.

We developed a novel experimental approach that uses an oscillating magnetic field to actively deform the contact region between a particle and a macrophage that is in the process of internalizing the particle by phagocytosis. By measuring the induced excursions of the particle, we determine the stiffness of the phagocytic cup quantitatively and with high temporal resolution. Our approach extends the general idea of optical magnetic twisting cytometry, a method that has previously been used to study the viscoelasticity of cytoskeletal networks [21], by adding rotational tracking at the single-cell level.

In this article, we present our method and the data we acquired on the evolution of translational and rotational stiffnesses during both successful and interrupted internalizations of particles. We found that during successful phagocytosis, the stiffness of the contact region between particle and cell first increases before peaking and converging to plateau values. During the uptake, the particle is accelerated and pulled towards the cell centre. In cases of interrupted internalization, the stiffness initially increases steeply, but then drops until the particle eventually detaches from the cell. Prior to detachment, the cell membrane undergoes strong bending deformations, indicating that the lipid bilayer has lost its association with the actin cortex. We interpret this effect as the forced breakdown of stalled phagocytic cups. Finally, to understand the obtained measurements quantitatively, we present a model of the phagocytic cup that describes the stiffness as a function of particle engulfment, and takes into account the deformation of the membrane and the elasticity of the underlying actin cortex. In the framework of this model, the peak in stiffness arises as the direct manifestation of the mechanical bottleneck that has been suggested as the origin of stalled phagocytic cups [10], and the slope of the increasing stiffness can be interpreted as the characteristic speed of membrane advancement.

2. Material and methods

2.1. Particle preparation

Ferromagnetic particles with a diameter of 4.5 μm (Spherotech, Lake Forest, IL, USA) were prepared as described previously [22]. Briefly, mouse immunoglobulin (IgG) from serum was covalently bound to the carboxyl-terminated particle surface by way of a two-step reaction based on 1-ethyl-3-(3-dimethylaminopropyl)carbodiimide and *N*-hydroxysuccinimide (all acquired from Sigma Aldrich, St. Louis, MO, USA). We used flow cytometry to verify that the particles were loaded with mouse IgG at saturating levels. To enable rotational particle tracking about three axes, the magnetic particles were subsequently labelled with fiducial fluorescent spheres (diameter 0.2 μm, Bangs Labs, Fisher, IN, USA) as previously described [22]. For experiments with a mixed functionalization with IgG and CD47, particles were prepared in a two-step procedure (see the electronic supplementary material for details).

2.2. Cell culture and sample preparation

Human acute monocytic leukaemia cells (THP-1) were cultured at 37°C in Roswell Park Memorial Institute medium (RPMI-1640, Life Technologies, Carlsbad, CA, USA) supplemented with 25 mM 4-(2-hydroxyethyl)-1-piperazineethanesulfonic acid buffer, GlutaMax-I, 10 per cent foetal calf serum (Life Technologies) and 1 per cent penicillin and streptomycin. Two days prior to an experiment, cells were seeded onto open fluid chambers and differentiated by addition of 160 nM phorbol-12-myristate-13-acetate (Sigma Aldrich) to the culturing medium (see the electronic supplementary material for details on fluid chamber assembly and sample preparation).

2.3. Magnetic actuation

Experiments were carried out on a magnetic quadrupole set-up as previously described by Janssen *et al*. [23] and used by Irmscher

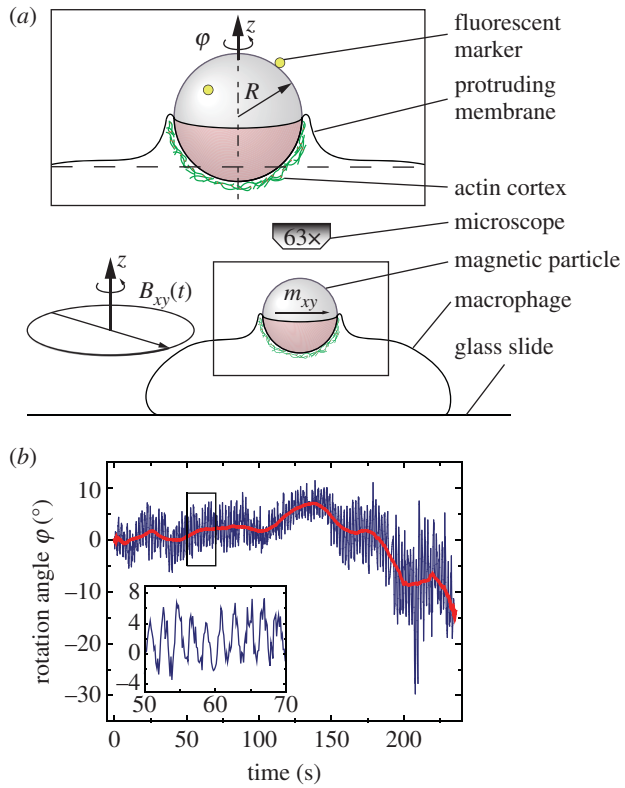

Figure 1. Experimental set-up and protocol. (*a*) Particles were functionalized with mouse IgG and allowed to bind to human macrophages adherent to a glass slide. The particles were magnetized in the *xy*-plane and subsequently actuated by a continuously rotating field in the same plane. In this way, particle drift around the *z*-axis could not lead to a change in torque. (*b*) The stiffness was calculated by evaluating the Fourier spectra of the angular displacements inside a moving window and by relating the amplitude to the applied magnetic torque. (Online version in colour.)

et al. [22]. Here, we used four pair-wise perpendicular coils to generate a rotating magnetic field in the plane of the sample (figure 1*a*). We conducted all of our experiments at a rotation frequency of 0.5 Hz and at magnetic flux densities ranging from 3.7 to 37 mT. As explained elsewhere [22], the generated field was homogeneous, with only minor lateral field gradients within the dimensions of the sample. Details are given in the electronic supplementary material.

2.4. Sample heating and image acquisition

The samples were kept at a constant temperature of about 37°C by a 180 µm thin transparent heater (Cell Micro Controls, Norfolk, VA, USA) that was placed underneath the sample. Imaging was performed on an upright microscope (Leica Microsystems, Wetzlar, Germany) at 63× magnification with a numerical aperture of the objective lens of 0.9 and at simultaneous fluorescence and bright-field illumination. The image acquisition was phase-locked to the magnetic actuation such that 15 frames were recorded during every actuation cycle. The acquired trajectories of translational and rotational displacements were Fourier transformed to determine the amplitude at the magnetic driving frequency. The magnetic torque has been measured by calibration in a viscous medium [22]. The stiffnesses were then calculated by dividing the applied magnetic torque by the Fourier components of the angular and translational displacements. The calculated rotational stiffness is a calibrated quantity. The translational stiffness has been normalized by the particle volume [21], but it is not a calibrated quantity because the translational motion is a higher order effect. We used the rotational stiffness for quantitative modelling and interpreted only relative changes of translational stiffness. Details about image acquisition and sample heating are given in the electronic supplementary material (movies from figures 2*a* and 3*a* are available at doi:10.5061/dryad.mh8c1).

2.5. Phagocytosis activity assays

To determine the global rate of particle uptake by the cells in a specific sample, we determined the ratio of internalized particles versus the total number of cell–particle contacts. After 45 min of contact between particles and cells, 5 µl of 2 mg ml^{-1} goat anti-mouse antibody with a fluorescent Alexa488 label (Life Technologies) were added to the chamber. To prevent further phagocytic activity, the sample was then incubated on ice for 30 min. After incubation, the sample was washed with copious amounts of cold Dulbecco's modified Eagle's medium. Finally, at least 80 cells were scored by counting the number of cell–particle contacts in bright-field mode and determining the fraction of internalized (i.e. non-fluorescent) particles.

3. Results

We introduced fluorescently tagged magnetic particles to fluid chambers containing adherent THP-1 macrophages and allowed the particles to bind. By imaging single particles in simultaneous bright-field and fluorescence mode, we then measured the translational and rotational stiffnesses of the dynamically changing contact interface between particles and cells.

3.1. Successful particle internalization

At the beginning of an experiment, a majority of particles was initially bound to the membranes of the cells, which can be attributed to the avid binding of the cellular FcR to the Fc regions of the immunoglobulins on the magnetic particles. In each sample, several phagocytosis events occurred during an experiment, and a limited number of internalization events could be recorded. We specifically picked particles that were marked by at least two clearly visible fluorescent markers to avoid misinterpretation of the rotational motion.

The rotating magnetic field caused the particles to undergo rotational as well as translational oscillations owing to the partial embedding of the particles in the cells. The obtained rotational and translational trajectories were processed by analysing the Fourier spectra inside a sweeping window function (figure 1*b*). As previously explained [22], the separate evaluation of rotational and translational oscillations is essential because the contact region between the particle and the cell is anisotropic. In the theory section of this article, we will present a model of a phagocytic cup that indeed predicts an anisotropic stiffness.

We monitored the stiffness during the internalization of particles in real time and found a characteristic evolution of the rotational stiffness k_φ and the translational stiffness G_{xy} (figure 2). Both stiffnesses are effective quantities that are determined by the geometry and the material properties of the binding site. The rotational stiffness initially increased slowly and intermittently reached local maxima during phases of increased velocity. Eventually, the rotational stiffness peaked and dropped off at a higher rate than it previously increased. The translational stiffness qualitatively followed a similar sequence, but its peak did not necessarily coincide with the peak of the rotational stiffness. At the end

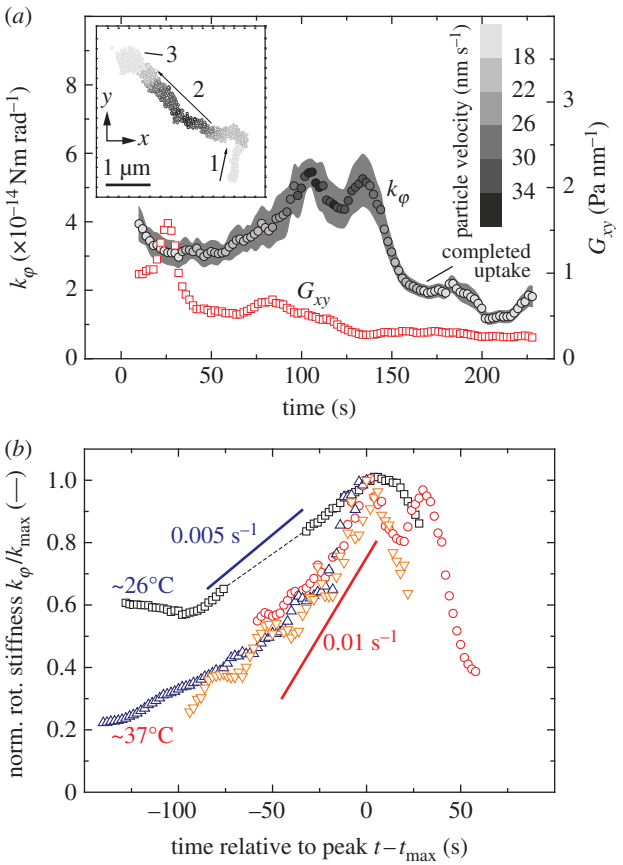

Figure 2. Temporally and spatially resolved evolution of stiffness during successful internalization. (*a*) Evolution of stiffness during engulfment of a single particle. During the internalization process, the stiffnesses and particle position are simultaneously tracked. The colour coding indicates the particle velocity. The inset shows the in-plane movement of the particle during the phagocytosis process and how it is pulled into its final position (sequence 1–3) at an accelerated pace. The main panel shows the simultaneous measurement of the translational (G_{xy}) and rotational (k_φ) stiffnesses. Characteristically, the rotational stiffness initially increases slowly and then drops off at a faster rate. The internalization is considered complete if both the rotational and the translational stiffnesses have peaked and converged to plateaus. Across cells, the phagocytosis events all exhibit an accelerated pull-in and show peaks in the stiffness evolutions, but the sequence of acceleration and peaks can be different. (*b*) Normalized rotational stiffness (norm. rot. stiffness) as a function of time relative to the peak. Whereas the absolute stiffness values can vary by one order of magnitude between cells, the shape of the peak of rotational stiffness is preserved. The superposition of normalized data from four internalizations shows good agreement in the slope leading up to the peak of stiffness. Note: some curves have gaps without measurement points (approx. 50 s) caused by timeslots of camera data retrieval. (Online version in colour.)

of the process, both the rotational and the translational stiffnesses converged to plateaus below their respective maximum values.

The rate at which the rotational stiffness increased before reaching the peak was well preserved across different cells. Figure 2 shows a comparison between four datasets that were recorded on different days. To extract the involved time scale, we normalized the data to the absolute stiffness at the peak of each curve and translated the curve such that the peak occurred at $t = 0$ s. Three curves were recorded at 37°C, with remarkable agreement of the slopes; the fourth curve was recorded at a temperature of about 26°C and showed a significantly lower slope.

Simultaneously, we monitored the overall trajectory of the phagocytic targets. Figure 2 shows the movement of the particle in the *xy*-plane with the colour-coded absolute velocity averaged over 20 s periods. The velocities but not the depicted positions have been corrected for motion of the cell itself. The data show that the particle moves towards the centre of the cell in almost a straight line at a non-constant velocity. The maximum particle velocity of about 35 nm s^{-1} is reached during the peak phase of the rotational stiffness. Note that this is the *xy*-component of the velocity and that the three-dimensional velocity can be larger. In other phagocytosis cases, the phase of increased velocity preceded the peak in stiffness.

We considered a particle successfully internalized if the translational and rotational stiffnesses stabilized, and did no longer change appreciably after a period that included the dynamic evolution shown in figure 2. In some cases, we observed that particles that had undergone this transition started rotating about the secondary axes after the particle reached its final position (see the electronic supplementary material, figure S2).

3.2. Interrupted internalization

In parallel to successful internalizations, we encountered particles whose uptake had begun but ultimately did not finish. We have recorded nine such cases where measurements show a sudden increase in rotational stiffness, followed by a short plateau and, eventually, the detachment of the particle (figure 3). In most of these cases, the particles had been bound to the apical membrane of the cells for periods of up to 30 min. At the beginning of a measurement, the rotational stiffness of the contact region between particle and cell membrane first remained constant. We observed nearly constant stiffness values for up to 200 s. Surprisingly, and initially without visible changes in the morphology of the cell, the stiffness then increased three to fivefold before peaking and proceeding to decrease. We found that the duration of the slope leading to the peak is about 30–50 s. This time was consistent across different cells and did not depend on the absolute stiffness that varied by one order of magnitude. On average, cases of interrupted phagocytosis were preceded by a fourfold increase of stiffness during a 60 s interval before the peak, whereas in successful events, the stiffness approximately doubled in the same time (figure 3*b*).

Typically, the stiffness peak was followed by a period wherein the stiffness decreased slowly with intermittent fluctuations. At the end of this intermediate phase, the oscillations of the particle rapidly increased. Interestingly, we found that this drop in stiffness was frequently accompanied by the gradual advent of conspicuous periodic deformations of distal parts of the cell body (see the electronic supplementary material, figure S3). When the particle finally detached, the edge of the cell often looked rugged, and occasionally we observed pieces of membrane material on the freely spinning particle.

3.3. Modelling the stiffness of a phagocytic cup

To understand our data quantitatively, we drew upon a model of a phagocytic cup developed by van Zon *et al.* [10] that describes the interaction potential between a particle and a cell membrane based on the elastic energy stored in the protrusion of the membrane. We extended this model to

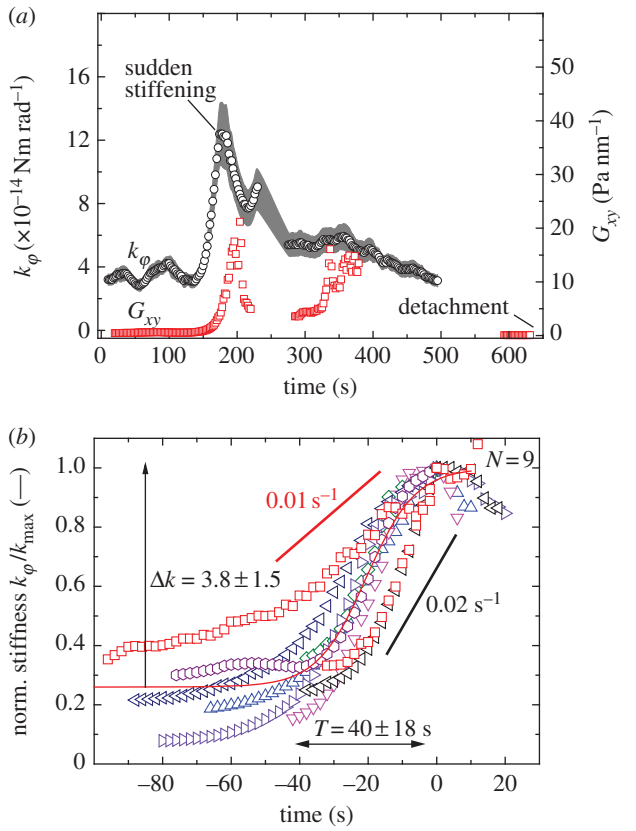

Figure 3. Evolution of stiffness during interrupted phagocytosis. (*a*) Initially, the rotational stiffness k_φ remains relatively unchanged, then it suddenly rises (at $t \sim 150$ s), it peaks (at $t \sim 180$ s) and then proceeds to fall off. At $t = 600$ s of the example, the particle was still loosely attached but underwent large excursions that prohibited rotational tracking. Shortly thereafter, the particle detached from the cell. The translational stiffness G_{xy} shows two peaks; in the second peak, the translational displacements were so small that they could not be accurately resolved. (*b*) Peak of rotational stiffness normalized with respect to the peak maximum. The rotational stiffness increases three to fivefold. The process takes about 30 to 50 s and is well preserved across cells ($N = 9$). The average rate (solid red (grey) line is the average of nine events) at which the stiffness increases in the final minute before reaching the peak is clearly higher than in cases of successful internalization (figure 2*b*). With one exception, all recorded cases of interrupted uptake are preceded by a more pronounced increase in stiffness. (Online version in colour.)

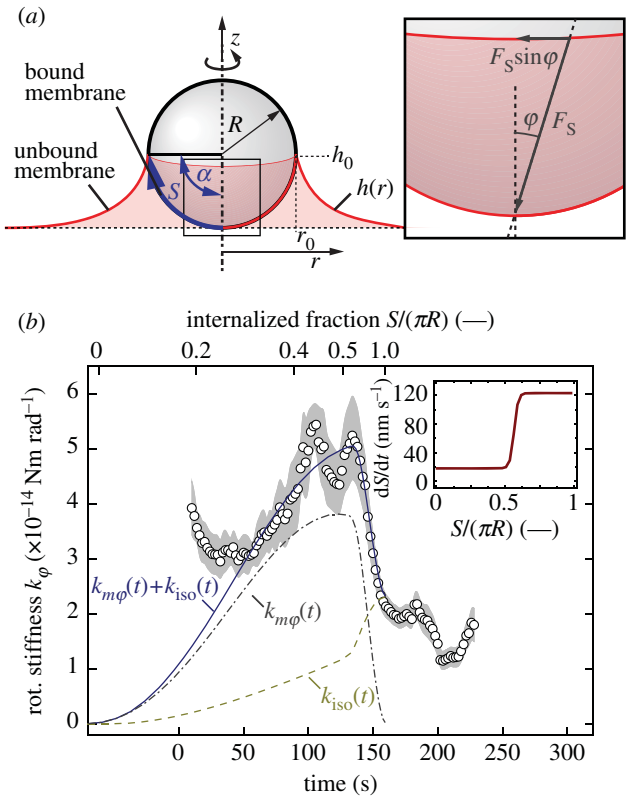

Figure 4. Modelling the stiffness of a phagocytic cup. (*a*) The protrusion of the membrane exerts a force F_S on the particle, similar to an extruded membrane tube. Twisting the phagocytic cup by a small angle φ results in a restoring force and a stiffness $k_{m\varphi}$ that oppose the externally applied magnetic torque. The magnitude of the torque depends on the force F_S and the position of the leading edge of the cup, indicated by the arc length $S = \alpha R$. (*b*) We model the total stiffness experienced by the particle as the sum of the membrane protrusion stiffness $k_{m\varphi}$ and an isotropic elastic stiffness k_{iso} that depends on the shear modulus of the actin cortex. (*b*, inset) The velocity first remains constant at about 20 nm s^{-1} and rises to about 120 nm s^{-1} at the point of half-engulfment. (Online version in colour.)

extract the apparent rotational stiffness of the phagocytic cup. Additionally, we had to account for the elastic potential of the contact region that we dynamically probed by actuation of the particles.

The formation of new bonds leads to an increase in the membrane area adherent to the particle. This wrapping process effectively restricts the motion of the particle inside a continuously steepening elastic potential that is dominated by the mechanical properties of the membrane and the underlying actin cortex. In this context, the bonds between the cell and the particle are considered infinitely stiff connections. Given the large number of available FcR and IgG molecules on the particles, several hundreds to thousands of bonds are expected to form during the engulfment of the particle. Magnetic actuation creates maximum shear forces of the order of 1 nN which, if evenly shared, results in an effective force per bond of the orders of a few piconewtons. This is not enough to break the bonds inside the phagocytic cup, especially in the face of rapid rebinding as a result of the actively driven protrusion of the membrane.

The model of van Zon *et al*. [10] describes the phagocytic cup as a radially symmetric protrusion of the membrane. The energy required to form the cup comes from the formation of bonds along the cell–particle interface and is described by the Helfrich free energy functional [24,25]

$$E = \int \mathrm{d}A(2\kappa H^2 + \sigma). \tag{3.1}$$

Here, H is the mean curvature, $\mathrm{d}A$ is a surface element, and κ and σ are the bending energy and surface tension of the cell membrane, respectively. The equilibrium shape $h(r)$ of the membrane between an attachment point (r_0,h_0) (figure 4*a*) at the circumference of the particle and an arbitrary cut-off radius is determined by minimizing the energy E.

Once the equilibrium shape for a specific position of the cell–particle contact line is known, the associated energy can be calculated using equation (3.1). Van Zon *et al*. [10] calculated the resistance against further extension of the membrane in terms of the force

$$F_S = \frac{\partial E}{\partial S}. \tag{3.2}$$

Here, $S = \alpha R$ is the arc length along the engulfed portion of the particle (figure 4). Because the membrane is attached to the particle, this force also acts on the particle and effectively draws it into the phagocytic cup. As the membrane advances,

the force increases because an increasingly large circumference has to be engulfed.

Starting from this model description, we derive the associated stiffness of the phagocytic cup. We consider the force F, a distributed line force acting along the leading edge of the membrane. If during actuation of the particle, the phagocytic cup is twisted around its z-axis by a small angle φ and no bonds are broken, the size of the cup and the force associated with it remain constant, but a restoring force will counteract the rotation of the particle (figure 4). The resulting torque on the particle is approximately

$$\tau_z = F_S R \sin\varphi \sin\alpha. \tag{3.3}$$

Under a small-angle approximation for φ, the stiffness around z hence becomes

$$k_{m\varphi} = \frac{\tau_z}{\varphi} \approx F_S R \sin\alpha. \tag{3.4}$$

This component of the stiffness has the character of a prestress as the force F_S does not depend on the deformation induced by the rotation of the particle.

In addition to this torque, the material surrounding the particle creates an elastic potential whose associated stiffness is determined by the degree of particle internalization. The problem of the apparent stiffness experienced by a partially embedded particle has been comprehensively treated by analytical and numerical methods [26,27]. Owing to the complexity of the cell structure, the probed region is mostly regarded as a homogeneous isotropic medium with shear modulus G. We have previously pointed out the pitfalls of this assumption [22], but we assume here that the connection between lipid bilayer and actin cortex is preserved throughout the internalization of the particle because (partial) disjoining would diminish the essential ability to exert force on the phagocytic target. Under this assumption, we based our calculation of the isotropic stiffness on the results of an finite-element method simulation carried out by Ohayon & Tracqui [27]. In their model, the particle is partially embedded in a hyperelastic (nonlinearly elastic; commonly used for biological materials) medium and undergoes both rotation and translation in response to an applied torque. The effective shear modulus can then be found by multiplying the material shear modulus G with an empirical expression that depends on the embedding angle α and the distance of the particle from the surface of the underlying substrate, h_u [27],

$$G_{iso} = \left(A(\alpha) + B(\alpha)\frac{2R}{h_u}\right)G. \tag{3.5}$$

Here, A and B are power series of the embedding angle. This effective shear modulus is then used to calculate the associated stiffness

$$k_{iso} = 6V\,G_{iso}, \tag{3.6}$$

where V is the volume of the particle.

The total stiffness experienced by a rotating particle is finally given by the linear superposition of the prestress component and the elastic stiffness of the emerging actin envelope,

$$k_\varphi = k_{m\varphi} + k_{iso}. \tag{3.7}$$

Our model does not include the dynamics of the growth of the phagocytic cup. However, the calculated values can be linked to our measurements by mapping the size parameter S onto a time scale, and by adjusting the parameters of the model such that the characteristic maxima and the rising slopes overlap. For this region of the dataset, we can then extract the approximate speed of cup advancement from the local value of dS/dt under the assumption that the cortical tension and the shear modulus are constant.

We applied our model to the dataset from figure 2 by assuming a cortical tension of $\sigma = 0.2\ \mathrm{mN\,m^{-1}}$ and a shear modulus of G=100 Pa (see §4 for rationale). Using these values, the peak stiffness is about $5 \times 10^{-14}\ \mathrm{Nm\,rad^{-1}}$. The slope leading to the peak overlaps with the measurements at a velocity of $dS/dt = 20\ \mathrm{nm\,s^{-1}}$. Upon reaching the peak, the rotational stiffness drops off at an approximately seven times higher rate than it increased before the peak. A comparison of the model with our data showed that the velocity increased to about $120\ \mathrm{nm\,s^{-1}}$. In the framework of this model description, the membrane hence first advances at a nearly constant speed from an initial embedding angle of about 50° at $t = 50$ s until it reaches the point of half-engulfment and proceeds to rapidly close the phagocytic cup. The normalized graph in figure 2*b* shows that throughout different cells, the speed of cup progression is remarkably well conserved at about $20\ \mathrm{nm\,s^{-1}}$. The measurement we recorded at 26°C shows a reduced speed of approximately $10\ \mathrm{nm\,s^{-1}}$.

3.4. Phagocytic activity assays

In microparticle experiments that involve the active induction of deformation, it is essential to study the potential interference of the particle actuation with the physiological processes. For example, the pulling velocity of filopodia has been shown to depend on the counteracting force exerted on the tip by an optically trapped particle [16]. In the context of our method, we decided to verify whether the oscillatory particle actuation has an influence on the internalization process.

We performed a series of assays designed to determine the binary outcome of phagocytosis at the single-cell level. We used secondary anti-mouse antibodies with an Alexa-488 label to distinguish internalized from non-internalized particles. The antibodies bind to external particles, but do not bind to particles inside cells. After incubation, we counted the number of internalized particles and related it to the total number of particle–cell contacts. We conducted this assay both for samples that had been incubated in the absence of magnetic actuation and for samples that had been subjected to magnetic particle actuation. The results show that under both conditions, about 60 per cent of all particles are internalized within a time window of 45 min (see the electronic supplementary material, figure S4). The degree of particle internalization was at or close to saturation, and the remaining 40 per cent are possibly cases of stalled phagocytosis. In fact, some of the particles scored as 'external' had a crescent shape in fluorescence, which indicates that the cell did not manage to fully engulf the respective particle. To test the validity of the assay itself, we performed additional tests at low temperature and in the presence of inhibitors cytochalasin D and CD47 (see the electronic supplementary material).

4. Discussion and conclusions

4.1. Measurement method

We present here a method to study the dynamic evolution of stiffness of a phagocytic cup during the uptake of a spherical

magnetic particle. To measure the stiffness, we use simultaneous bright-field and fluorescence imaging, and track the motion of the particle in an oscillating magnetic field. The stiffness and its changes are a consequence of the increasingly protruding membrane that restricts the motion of the particle. Our method allows us to detect the internalization of a particle based on its motion and the associated stiffness, without the need for fluorescent labelling of the cell membrane.

Previous research into the mechanical aspects of phagocytosis has focused on the extracellular transport by extended filopodia [16], on the viscoelasticity of the cytoplasm [18] or on the global change in surface tension during particle internalization [11,15,28]. To our knowledge, our approach for the first time allows localized quantitative measurements of the mechanics of the phagocytic cup progression, thereby filling a gap in the temporal sequence of events during internalization.

In the context of phagocytosis, magnetic tweezers have been used to exert pulling forces on externally bound particles. While such approaches are suitable for studying the viscoelastic properties of the actin cortex, they are prone to disturb the formation of the phagocytic cup because the vector of the applied force is nearly anti-parallel to the preferred pull-in direction of the particle. By applying a continuously rotating 'tickling field', we apply a shear force that is perpendicular to the symmetry axis of the phagocytic cup (if the particle is not taken up 'sideways'), and hence less likely to disturb the physiological activity of the cell.

To confirm that the application of a magnetic tickling field indeed does not affect the efficiency of phagocytosis, we performed assays to measure the binary outcome of particle binding at the single-particle level. These assays showed no significant difference in phagocytic efficiency between samples that had been incubated under control conditions and those that had been exposed to magnetic actuation. While this result proves that our method does not significantly hinder phagocytosis, it also indicates that phagocytosis is not facilitated by the application of force. While less intuitive than a detrimental effect, the application of force at the micro-scale has been shown to elicit strengthening of the underlying cytoskeletal structures [29,30]. In the context of phagocytic uptake, such behaviour has (to our knowledge) not been reported.

To further improve our method, it can be integrated with direct (confocal) imaging of the proteins involved in shaping the phagocytic cup, as their spatial and temporal organization is tied to the parameters we assume here to be constant. To increase the throughput of our method, e.g. to enable population studies, our technique has to be integrated with a method that allows control of the initiation of contact between single particles and cells. This can be achieved by using a multi-chamber microfluidic system or by using a weak optical trap to establish contact between particles and cells.

4.2. Observation of internalization

During internalization, an initially bound particle moves to a position within the perimeter of the cell. The fact that the outline of the particle is fully enclosed by the cell does not necessarily indicate finalized uptake because we have observed that a particle reached a final position before the rotational stiffness peaked. Extracellular transport of the particle, e.g. by contraction, and its engulfment can thus be independent events that can proceed simultaneously or sequentially.

Because the extent of the phagocytic cup could not be visualized directly, finalized uptake of the particle had to be determined from the associated secondary measurements. As mentioned above, one criterion was the cell-induced displacement of the particle. This movement could be less pronounced in cases where the measurement was started after the particle had already been pulled closer. A second criterion was the observation of a peak in rotational stiffness, followed by a drop and stabilization at a lower level. Whether both rotational and translational stiffnesses decreased by an equal factor presumably depended on the way the nascent phagosome latched onto the cytoskeletal support structures. The emergence of strong rotations about secondary axes at nearly constant translational stiffness was seen as a clear sign of finished phagocytosis. We attribute this observation to the fact that the phagosome has an increased rotational freedom within the cytoplasm when the connection to the cell membrane is lost (see the electronic supplementary material, figure S2 for an example).

Our measurements reveal that the measured translational and rotational stiffness are not synchronous and peak at different times. From previous studies [27], it is known that the partial engulfment of a particle imposes kinematic constraints on its motion under an applied magnetic torque. The relationship between translational and rotational motion is nonlinear, and as a result, there is a nonlinear relationship between the associated stiffnesses that at any moment in time is determined by the instantaneous embedding angle. Because in our experiments the torque on the particle is calibrated only for rotation about the z-axis, we cannot quantitatively analyse the relationship between G_{xy} and k_{φ}.

4.3. Interrupted internalization

At first glance, the evolutions of stiffness in cases of interrupted and successful internalization seem similar, as the stiffness first peaks before dropping precipitously. However, in cases of interrupted internalization, both the translational and rotational stiffness do not reach a plateau after peaking. Instead, they concomitantly proceed to drop until the particle detaches. This is in contrast to successful internalizations, where the translational and rotational stiffnesses converge to new levels. During interrupted internalizations, bonds between the particle and the cell membrane are broken and, as indicated by the onset of strong membrane fluctuations, the link between lipid bilayer and actin cortex is severed.

At the start of experiments that culminated in particle detachment, the rotational and translational stiffnesses often remained comparatively constant for observed periods of up to 4 min. The internalization of particles and bacteria is known to stall, even under physiological conditions [10,31]. This has been explained by invoking the idea of a mechanical bottleneck [10] that sets a limit to the extrusion of the membrane, and is determined by the size and orientation of the phagocytic target and the potential of the cell to generated force by the directed polymerization of actin. In the context of our experiments, the extended period of nearly constant stiffness at the start of an experiment hence likely indicates that the phagocytic cup has stalled.

The dramatic increase in stiffness is in these cases presumably not caused by a rapid advance of the membrane. While the onset of phagocytosis immediately after formation of the first bonds is known to be occasionally delayed, the process

itself proceeds continuously until it either finishes or stalls. The unfolding of membrane wrinkles is one process by which cells increase their available surface area during the late stages of the uptake phase [12,32]. Because this process involves the irreversible breaking of bonds and a change in surface area, it has previously been modelled as a viscous contribution to the cortical tension [11]. The unfolding of wrinkles and the subsequent increase in surface area would hence lead to a transient rise of the effective cortical tension and the associated stiffness.

4.4. Linking results and theory

Our measurements show that the rotational stiffness peaks during the internalization of a particle. This is not obvious as conventional continuum mechanics models predict that an increasingly embedded particle experiences a monotonously rising stiffness. However, in FcR-mediated phagocytosis, a protrusion of the membrane grows around the target. Because this protrusion is stabilized by bonds, the particle experiences a growing force in vertical direction. As pointed out by van Zon *et al*. [10], this force becomes maximal when the leading edge of the membrane extends to the equator of the particle. We treat this force as a prestress that is independent of the deformation induced by actuation. Under small torsional deformations, the shearing of the force field then gives rise to a restoring torque on the particle. Within this framework, the measured peak in stiffness could thus be seen as direct evidence of a mechanical bottleneck. It is also instructive to consider the model of a hyperboloid for comparison (see the electronic supplementary material, figure S5).

The prestress in the membrane depends on the bending energy and the effective cortical tension of the composite bilayer–cortex assembly. In line with previous findings [10,33], we assumed a value of 1×10^{-18} J for the bending stiffness of the bilayer–cortex assembly. We used the resting tension of suspended J774 macrophages (0.14 mN m^{-1} [32]) as a point of reference for our model. The value of the cortical tension is likely only constant on short time segments, such as the characteristic region around the peak of stiffness.

In addition to the torque from the prestress in the membrane, the particle experiences an elastic restoring torque as the actin cortex is deformed by actuation. To find appropriate model parameters, we refer to magnetic microrheology studies [34,35] which have found that the shear modulus of the actin cortex of endothelial cells is of the order of 100 Pa under baseline conditions. The model we adapted from van Zon *et al*. [10] takes the increase of actin concentration into account by assuming that the energy of the bound membrane is increased by a factor of five with respect to that of the unbound membrane. In the later stages of the internalization, the effective shear modulus is thought to be increasingly determined by the mechanical linkage between the phagosome and the cytoskeleton.

Our description of the stiffness of a phagocytic cup leads to an interesting prediction about the internalization of particles coated with complement. Previously, those particles have been said to 'sink' into the cell [3,4,36], i.e. without the formation of a membrane protrusion. Considering our two-component model, the evolution of stiffness in those cases should thus display a less pronounced maximum, but instead mainly reflect the change in effective shear modulus of the surrounding medium as the particle is internalized.

Our model also implies that the stiffness of the contact interface is anisotropic because the membrane deformation creates a state of uniaxial prestress that is superposed onto the elasticity of the material (which in itself is not necessarily isotropic). This idea is depicted in the electronic supplementary material, figure S6.

Our measurements are in agreement with the calculated model values when the cup grows at a constant velocity before the stiffness reaches its peak and accelerates after passing the maximum. From the superposition of size and time scales, we could extract the effective speed at which the phagocytic cup grows around the particle. As the protrusion is driven by the directed polymerization of actin, the speed at which the cup advances is directly related to the counteracting force that the membrane exerts on the growing ends of the filaments. We used the Brownian ratchet model to obtain an estimate of the number of actin filaments required to push out the membrane and to reason that the derived speed of cup advancement of about 20 nm s^{-1} is realistic (see the electronic supplementary material).

4.5. Concluding remarks

Our experimental method and theoretical framework constitute a novel approach to study the mechanics of phagocytic cup formation at the single-cell level in real time. We think that the approach is suitable to study the influence of uptake inhibitors on the dynamics of phagocytic cup formation. For example, CD47 has recently been identified as a membrane marker whose presence on phagocytic targets decreases the efficiency of uptake by suppression of myosin activity [31,37]. While the inhibiting effect of CD47 has been studied [31], it is not clear how it affects the mechanics of phagocytic cup formation.

This research was performed within the framework of CTMM, the Center for Translational Molecular Medicine (www.ctmm.nl), project CIRCULATING CELLS (grant no. 01C-102), and supported by the Dutch Heart Foundation. The research was also supported by the BioNano Center of Excellence of the Dutch 3TU federation. M.W.J.P. is an employee of Philips Research.

References

1. Desjardins M, Houde M, Gagnon E. 2005 Phagocytosis: the convoluted way from nutrition to adaptive immunity. *Immunol. Rev.* **207**, 158–165. (doi:10.1111/j.0105-2896.2005.00319.x)
2. Vogel G, Thilo L, Schwarz H, Steinhart R. 1980 Mechanism of phagocytosis in *Dictyostelium discoideum*: phagocytosis is mediated by different recognition sites as disclosed by mutants with altered phagocytotic properties. *J. Cell Biol.* **86**, 456–465. (doi:10.1083/jcb.86.2.456)
3. Underhill DM, Goodridge HS. 2012 Information processing during phagocytosis. *Nat. Rev. Immunol.* **12**, 492–502. (doi:10.1038/nri3244)
4. Aderem A, Underhill DM. 1999 Mechanisms of phagocytosis in macrophages. *Ann. Rev. Immunol.* **17**, 593–623. (doi:10.1146/annurev.immunol.17.1.593)
5. Hoppe AD, Swanson JA. 2004 Cdc42, Rac1, and Rac2 display distinct patterns of activation during phagocytosis. *Mol. Biol. Cell* **15**, 3509–3519. (doi:10.1091/mbc.E03-11-0847)
6. Hunter S, Kamoun M, Schreiber AD. 1994 Transfection of an Fcy receptor cDNA induces T cells

to become phagocytic. *Proc. Natl. Acad. Sci. USA* **91**, 10 232–10 236. (doi:10.1073/pnas.91.21.10232)

7. Griffin Jr FM, Griffin JA, Leider JE, Silverstein SC. 1975 Studies on the mechanism of phagocytosis I. Requirements for circumferential attachment of particle-bound ligands to specific receptors on the macrophage plasma membrane. *J. Exp. Med.* **142**, 1263–1282. (doi:10.1084/jem.142.5.1263)
8. Swanson JA, Johnson MT, Beningo K, Post P, Mooseker M, Araki N. 1999 A contractile activity that closes phagosomes in macrophages. *J. Cell Sci.* **112**, 307–316.
9. Tollis S, Dart AE, Tzircotis G, Endres RG. 2010 The zipper mechanism in phagocytosis: energetic requirements and variability in phagocytic cup shape. *BMC Syst. Biol.* **4**, 1–17. (doi:10.1186/1752-0509-4-1)
10. Van Zon JS, Tzircotis G, Caron E, Howard M. 2009 A mechanical bottleneck explains the variation in cup growth during FcγR phagocytosis. *Mol. Syst. Biol.* **5**, 1–12. (doi:10.1038/msb.2009.59)
11. Herant M, Heinrich V, Dembo M. 2005 Mechanics of neutrophil phagocytosis: behavior of the cortical tension. *J. Cell Sci.* **118**, 1789–1797. (doi:10.1242/jcs.02275)
12. Hallett MB, Dewitt S. 2007 Ironing out the wrinkles of neutrophil phagocytosis. *Trends Cell Biol.* **17**, 209–214. (doi:10.1016/j.tcb.2007.03.002)
13. Beningo KA, Wang Y-L. 2002 Fc-receptor-mediated phagocytosis is regulated by mechanical properties of the target. *J. Sci.* **115**, 849–856.
14. Evans E, Leung A, Zhelev D. 1993 Synchrony of cell spreading and contraction force as phagocytes engulf large pathogens. *J. Cell Biol.* **122**, 1295–1300. (doi:10.1083/jcb.122.6.1295)
15. Lee C-Y, Herant M, Heinrich V. 2011 Target-specific mechanics of phagocytosis: protrusive neutrophil response to zymosan differs from the uptake of antibody-tagged pathogens. *J. Cell Sci.* **124**, 1106–1114. (doi:10.1242/jcs.078592)
16. Kress H, Stelzer EHK, Holzer D, Buss F, Griffiths G, Rohrbach A. 2007 Filopodia act as phagocytic tentacles and pull with discrete steps and a load-dependent velocity. *Proc. Natl. Acad. Sci. USA* **104**, 11 633–11 638. (doi:10.1073/pnas.0702449104)
17. Vonna L, Wiedemann A, Aepfelbacher M, Sackmann E. 2007 Micromechanics of filopodia mediated capture of pathogens by macrophages. *Eur. Biophys. J.* **36**, 145–151. (doi:10.1007/s00249-006-0118-y)
18. Shekhar S, Cambi A, Figdor CG, Subramaniam V, Kanger JS. 2012 A method for spatially resolved local intracellular mechanochemical sensing and organelle manipulation. *Biophys. J.* **103**, 395–404. (doi:10.1016/j.bpj.2012.06.010)
19. Wilhelm C, Gazeau F, Bacri J-C. 2003 Rotational magnetic endosome microrheology: viscoelastic architecture inside living cells. *Phys. Rev. E* **67**, 1–12. (doi:10.1103/PhysRevE.67.061908)
20. Valberg PA, Feldman HA. 1987 Magnetic particle motions within living cells. Measurement of cytoplasmic viscosity and motile activity. *Biophys. J.* **52**, 551–61. (doi:10.1016/S0006-3495(87)83244-7)
21. Fabry B, Maksym G, Butler J, Glogauer M, Navajas D, Fredberg J. 2001 Scaling the microrheology of living cells. *Phys. Rev. Lett.* **87**, 1–4. (doi:10.1103/PhysRevLett.87.1)
22. Irmscher M, De Jong AM, Kress H, Prins MWJ. 2012 Probing the cell membrane by magnetic particle actuation and Euler angle tracking. *Biophys. J.* **102**, 698–708. (doi:10.1016/j.bpj.2011.12.054)
23. Janssen XJA, Van Reenen A, Van IJzendoorn LJ, De Jong AM, Prins MWJ. 2011 The rotating particles probe: a new technique to measure interactions between particles and a substrate. *Colloids Surf. A Physicochem. Eng. Aspects* **373**, 88–93. (doi:10.1016/j.colsurfa.2010.10.033)
24. Helfrich W. 1973 Elastic properties of lipid bilayers: theory and possible experiments. *Z. Naturforsch.* **28c**, 693–703.
25. Boal D. 2008 *Mechanics of the cell*, 1st edn. Cambridge, UK: Cambridge University Press.
26. Ohayon J, Tracqui P, Fodil R, Féréol S, Laurent VM, Planus E, Isabey D. 2004 Analysis of nonlinear responses of adherent epithelial cells probed by magnetic bead twisting: a finite element model based on a homogenization approach. *J. Biomech. Eng. Trans. ASME* **126**, 685–698. (doi:10.1115/1.1824136)
27. Ohayon J, Tracqui P. 2005 Computation of adherent cell elasticity for critical cell-bead geometry in magnetic twisting experiments. *Ann. Biomed. Eng.* **33**, 131–141. (doi:10.1007/s10439-005-8972-9)
28. Herant M, Heinrich V, Dembo M. 2006 Mechanics of neutrophil phagocytosis: experiments and quantitative models. *J. Cell Sci.* **119**, 1903–1913. (doi:10.1242/jcs.02876)
29. Roca-Cusachs P, Gauthier NC, Sheetz MP. 2009 Clustering of $\alpha5\beta1$ integrins determines adhesion strength whereas $\alpha V\beta3$ and talin enable mechanotransduction. *Proc. Natl Acad. Sci. USA* **106**, 16 245–16 250. (doi:10.1073/pnas.0902818106)
30. Wang N, Butler JP, Ingber DE. 1993 Mechanotransduction across the cell surface and through the cytoskeleton. *Science* **260**, 1124–1127. (doi:10.1126/science.7684161)
31. Tsai RK, Discher DE. 2008 Inhibition of 'self' engulfment through deactivation of myosin-II at the phagocytic synapse between human cells. *J. Cell Biol.* **180**, 989–1003. (doi:10.1083/jcb.200708043)
32. Lam J, Herant M, Dembo M, Heinrich V. 2009 Baseline mechanical characterization of J774 macrophages. *Biophys. J.* **96**, 248–254. (doi:10.1529/biophysj.108.139154)
33. Simson R, Wallraff E, Faix J, Niewöhner J, Gerisch G, Sackmann E. 1998 Membrane bending modulus and adhesion energy of wild-type and mutant cells of *Dictyostelium* lacking talin or cortexillins. *Biophys. J.* **74**, 514–522. (doi:10.1016/S0006-3495(98)77808-7)
34. Feneberg W, Aepfelbacher M, Sackmann E. 2004 Microviscoelasticity of the apical cell surface of human umbilical vein endothelial cells (HUVEC) within confluent monolayers. *Biophys. J.* **87**, 1338–1350. (doi:10.1529/biophysj.103.037044)
35. Bausch AR, Ziemann F, Boulbitch AA, Jacobson K, Sackmann E. 1998 Local measurements of viscoelastic parameters of adherent cell surfaces by magnetic bead microrheometry. *Biophys. J.* **75**, 2038–2049. (doi:10.1016/S0006-3495(98)77646-5)
36. Allen LA, Aderem A. 1996 Molecular definition of distinct cytoskeletal structures involved in complement- and Fc receptor-mediated phagocytosis in macrophages. *J. Exp. Med.* **184**, 627–637. (doi:10.1084/jem.184.2.627)
37. Tsai RK, Rodriguez PL, Discher DE. 2010 Self inhibition of phagocytosis: the affinity of 'marker of self' CD47 for SIRPalpha dictates potency of inhibition but only at low expression levels. *Blood Cells Mol. Dis.* **45**, 67–74. (doi:10.1016/j.bcmd.2010.02.016)